# Post polymerisation hypercrosslinking with emulsion templating for hierarchical and multi-level porous polymers

Amadeja Koler[a], Irena Pulko[b], Peter Krajnc[a]

[a]University of Maribor, Faculty of Chemistry and Chemical Engineering, PolyOrgLab, Smetanova 17, Maribor, Slovenia

[b]Faculty of Polymer Technology, Ozare 19, Slovenj Gradec, Slovenia

**Key words: polyHIPE; hypercrosslinking; porous polymers; porosity; emulsion templating; hierarchical polymers**

## Abstract

Porosity in polymers and polymeric materials adds to their functionality due to achieving the desired tailored characteristics. Therefore, applications in many fields, e.g. catalysis, separation, solid phase synthesis, adsorption, sensing, biomedical devices etc., drive the development of polymers with controlled morphology in terms of pore size, shape, interconnectivity and pore size distribution. Of particular interest are polymers with distinct bimodal or hierarchical pore distribution as this enables uses in applications where pore sizes on multiple levels are needed. Emulsion templating can be used for the preparation of polymers with included interconnected spherical pores on the micrometre level while post polymerisation crosslinking adds micro porosity. Combined use of both techniques yields interesting materials with great application potential.

## 1. Introduction

Methods for generation of porosity in polymers can be generally divided into chemical and physical. Among physical methods, various templating can be used while post polymerisation crosslinking and phase separation induced syneresis are examples of chemical methods (Figure 1). According to IUPAC guidelines [1], pores are referred to as macro (diameters over 50 nm), meso (diameters between 2 and 50 nm) and micro (diameters less than 2 nm). Among templating methods, emulsion templating is widely used [2–7]. Both water-in-oil and oil-in-water emulsions can be used for the purpose of macro porosity induction during the polymerisation process. When a high concentration of the droplet phase is used, droplets' shapes become distorted and a dispersion of droplet size is observed (Figure 2). In the case of inclusion of monomers into the continuous phase the polymerisation results in a monolithic porous material, typically with an interconnected porosity which is the result of the shrinkage of continuous phase volume at the sol-gel transition. In the case of uniform packing of monodisperse spherical droplets, the volume of the droplet phase accounts for 74,05% of the total emulsion volume while at random packing this share is lower, namely 64% [8]. Polymers prepared from emulsions with droplet phase volume shares higher than these border values are termed polyHIPEs, following the abbreviation for high internal phase emulsion [9]. The internal topology of so prepared polymeric material features two levels of pores, the primary pores, termed cavities and secondary, interconnecting pores (Figure 3). The size of primary pores follows the size of the droplets prior to polymerisation as demonstrated by a series of experiments containing emulsion aging and room temperature polymerisation initiation with a redox initiation pair [10]. Therefore, the control of emulsion droplet size prior to polymerisation is the main control also for the primary pore size. The main factors controlling emulsion droplet size include emulsion stabilization by surfactant molecules and energy input at emulsion preparation.

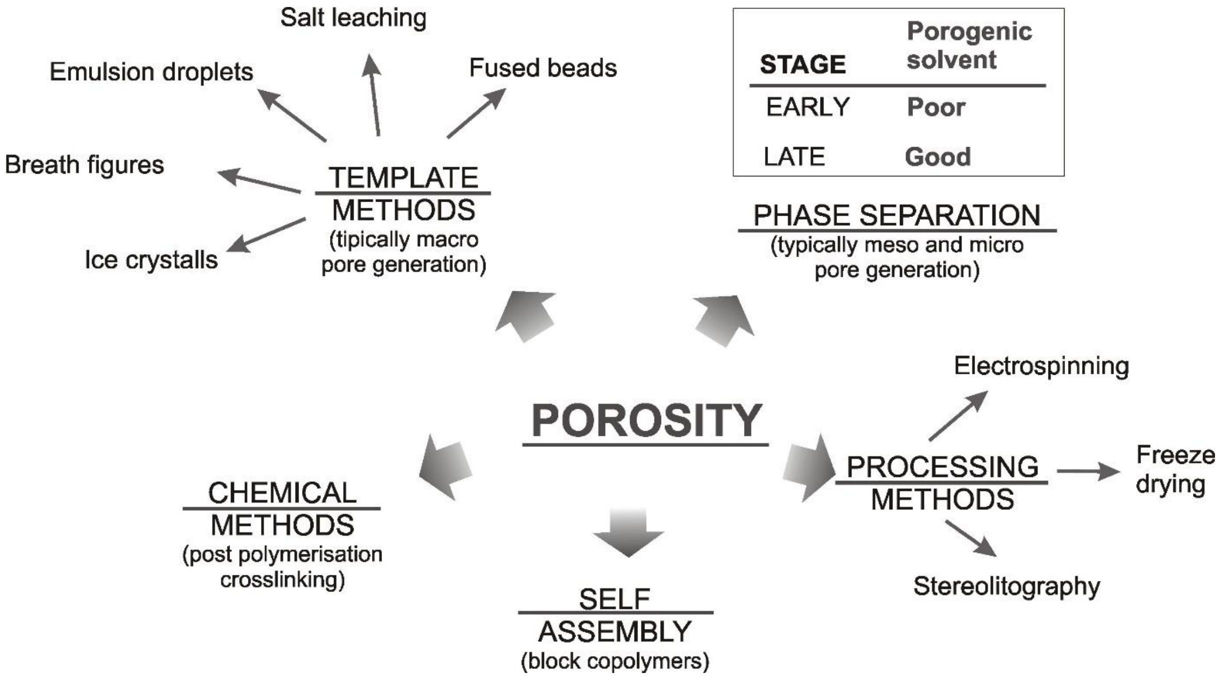

**Figure 1**: Methods for porosity creation in polymers

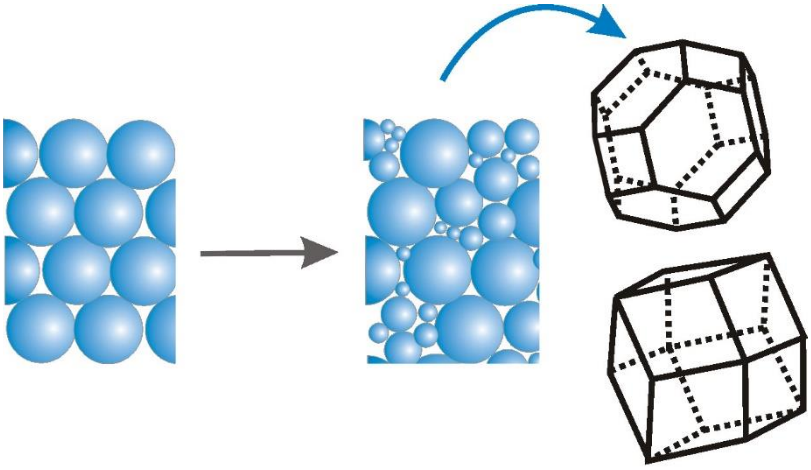

**Figure 2**: Droplet size and shape change at emulsion concentration

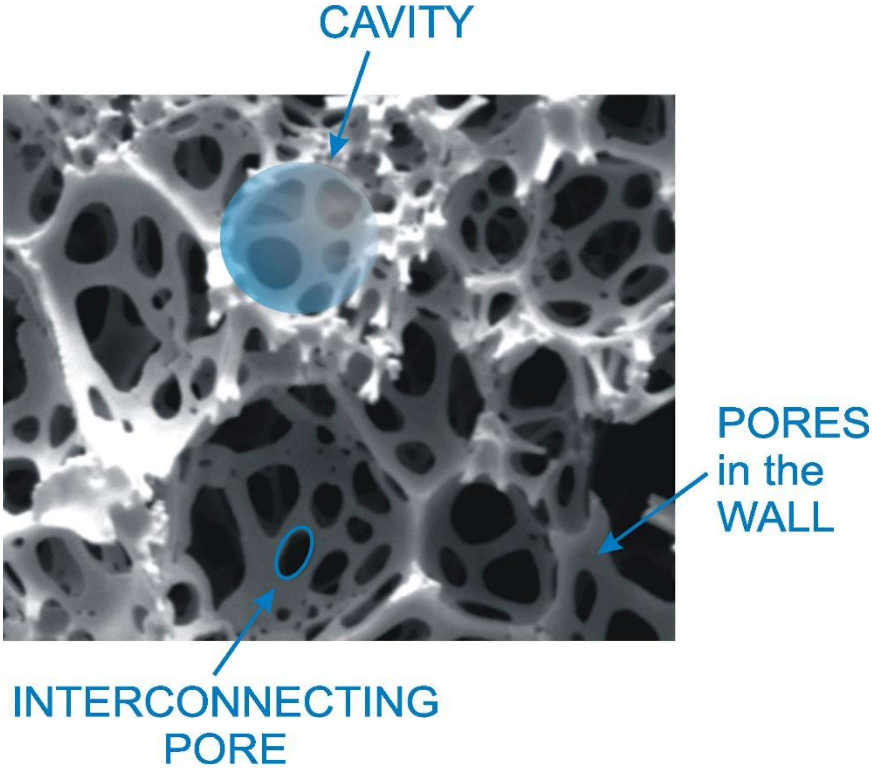

**Figure 3**: PolyHIPE morphology

On the other hand, the frequency and size of interconnecting pores determine the connectivity of porous structure or what could be defined as the *openness* of the structure (Figure 4) [11].

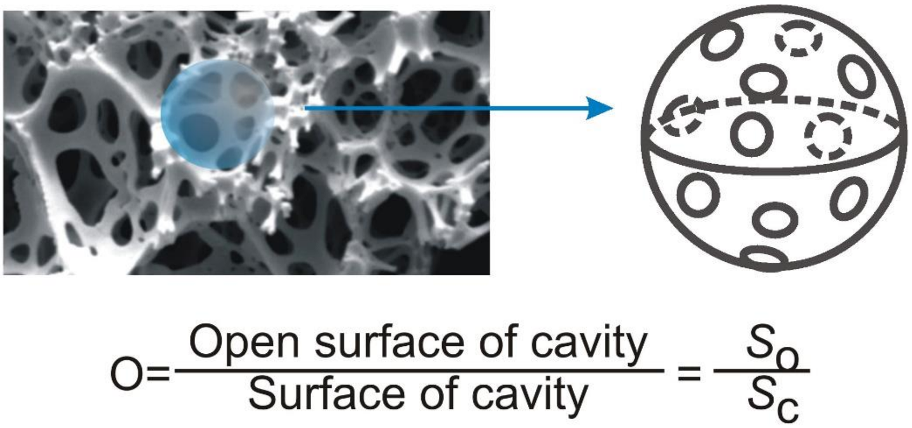

$$O = \frac{\text{Open surface of cavity}}{\text{Surface of cavity}} = \frac{S_O}{S_C}$$

**Figure 4**: Interconnectivity of porous structure in polyHIPEs

The thickness of the film of continuous phase between the adjacent droplets seems to be the main factor affecting the size and frequency of the interconnecting pores. This is mainly determined by the droplet to continuous phase volume ratio and by the concentration and structure of the surfactant(s). In summary, main factors determining the morphological features of polyHIPEs are volume ratio of droplet/continuous phase, energy input at preparation, and surfactant concentration and structure. Many other variables were considered and their role can be important. This makes a polymerizable HIPE a multi variable system and careful experimental consideration must be involved when planning a particular structure (Figure 5).

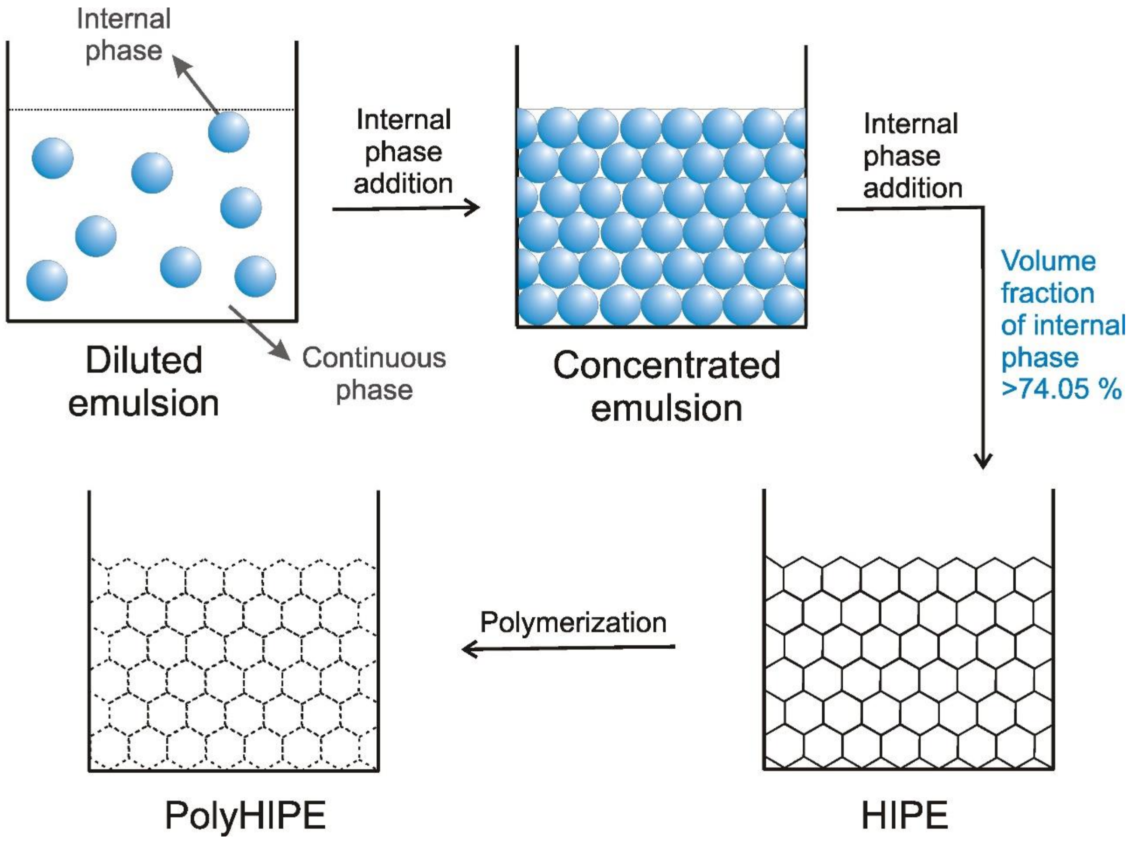

**Figure 5**: polyHIPE preparation

## 2. Recent advances in polyHIPE synthesis and creation of multi-level porosity

While water-in-oil high internal phase emulsions are most commonly used for the preparation of polyHIPE polymers, other emulsion based systems have also been described. Both oil-in-water and oil-in-oil high internal phase emulsions can be applied [12]. For water soluble or hydrophilic monomers, solvents such as hydrocarbons or benzene derivatives were used as the droplet phase. In such manner, polyHIPEs were prepared from acrylic acid [13], 2-hydroxyethyl methacrylate [14–18], *N*-isopropyl acrylamide (NiPAAm) [19,20], acrylamide [21], 1-vinyl-5-aminotetrazole [22,23], and dimethylaminoethyl methacrylate [24].

Furthermore, combination of emulsion templating and other porosity induction techniques, have yielded hierarchically porous polymer materials. Sušec et al. [25] and Johnson et al. [26] have demonstrated the principle of applying a high internal phase emulsion within a stereophotolithographic based additive manufacturing setup. With such a system, a three dimensional object can be built with a lithographic photo polymerizable system however due to the use of a high internal phase emulsion with photo polymerizable monomers in the continuous phase, the object has an internal polyHIPE structure. Thus, another level of porosity is created using the lithographic process while pores of smaller dimensions are created as a result of emulsion templating. Monomer mixtures particularly suitable for such photo polymerisation were found to be multifunctional thiols and alkenes producing polymer networks via the thiol-ene click reaction [27].

Another recent example of adding structure complexity is the use of hard sphere templating. Within this approach, spherical particles (typically polymeric) are fused together, to construct a monolithic porous network with interconnected porosity. So constructed material is then impregnated with a monomer mixture, polymerized while the previously constructed template dissolved. Macroporous polymethacrylates prepared in this way have open interconnected porosity and have been used as scaffolds in tissue engineering applications [28–31]. We have shown that a combination of this hard sphere templating and high internal phase emulsion templating can yield polymers with open interconnected and hierarchical porosity which is especially advantageous in biomedical applications such as tissue constructs [32]. Primary monolithic template was formed by sintering polymethyl methacrylate beads and subsequently filled with a high internal phase emulsion containing thiols and alkenes as monomers in the continuous phase (Figure 6). Photopolymerisation yielded hierarchically structured polymer network with open porosity and biodegradability was introduced by the use of thiol monomers with ester groups. (Figure 7) So prepared multi-level porous polymers were successfully applied as scaffolds for human bone cell growth.

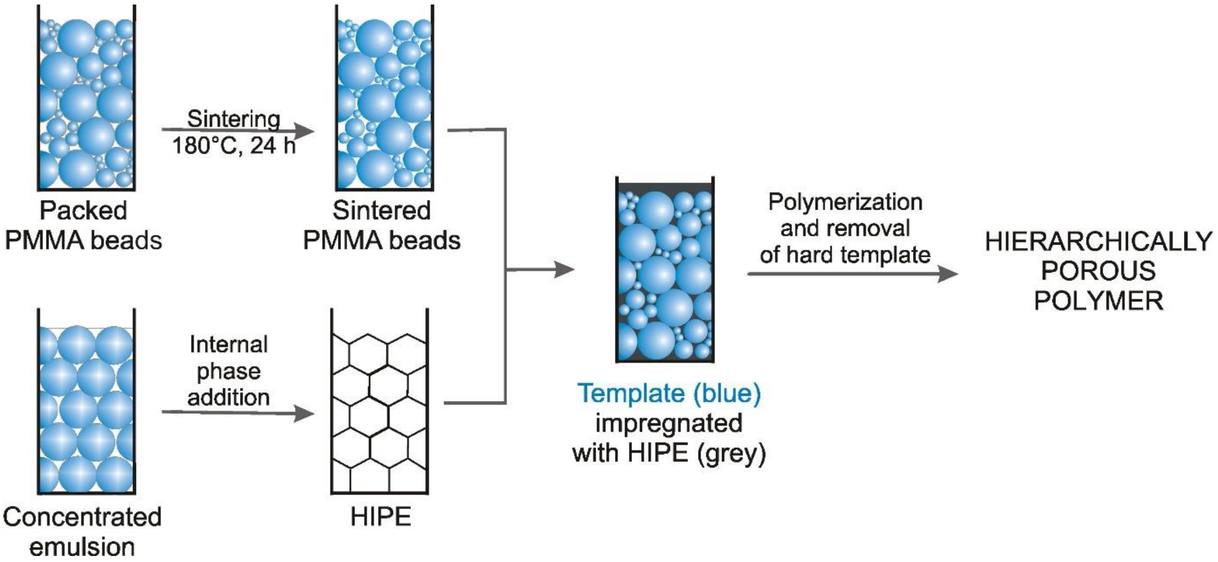

**Figure 6**: Combination of hard sphere and emulsion templating

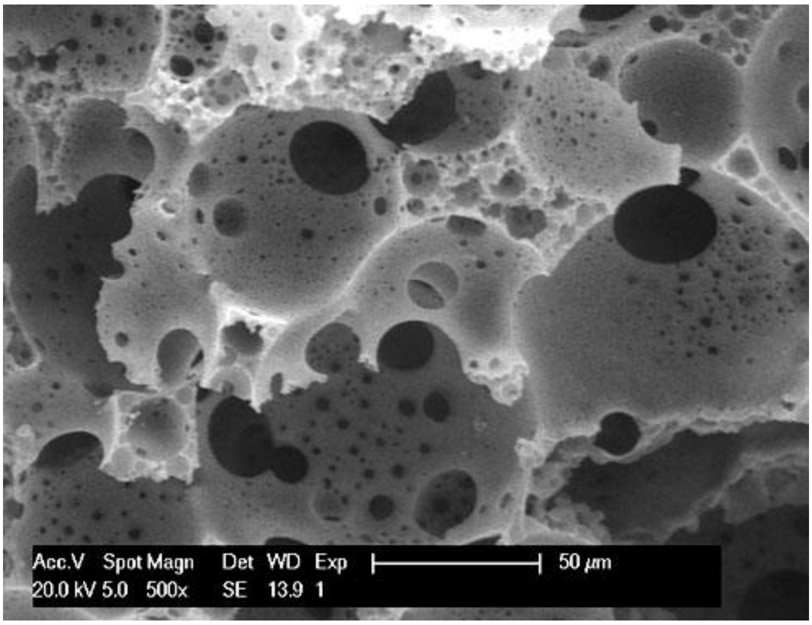

**Figure 7**: Scanning electron micrograph of hierarchically porous polymer prepared by combining hard sphere and emulsion templating

While electrospinning is in itself a method producing porous fibrous structures from polymer solutions or melts [33,34], high internal phase emulsion templating has been used in combination with electrospining to add a level of porosity to the product [35,36]. Using this combination, fibres with bicontinuous morphology were obtained by elecrospinning HIPEs consisting of aqueous poly(vinyl alcohol) solutions dispersed within polycaprolactone-in-toluene solutions[35]. Similarly, Dikici et al.[36] used a polycaprolactone barrier membranes to form bilayers by combining electrospinning and emulsion templating techniques and applied them for guided bone regeneration. The electrospunn fibres had a mixture of open and closed cell porous polyHIPE type morphology.

## 3. Inducing meso and micro porosity within polyHIPEs

Due to relatively large pores induced by the droplet phase in polyHIPE preparation, the result is a macroporous material with primary pore sizes typically between 500 nm and 100 μm. Consequently, specific surface areas of polyHIPEs are low, usually below 50 $m^2$/g. This is the result of the lack of meso and micro porosity. For many applications surface area of the polymer support plays a vital role. Early attempts of improving specific surface areas of polyHIPEs mostly included the addition of porogenic solvents to the monomer containing continuous phase [37] and increasing the crosslinking degree [38] thus producing polyHIPEs with specific surface areas up to 550 $m^2/g$. Introduction of porogenic solvent into the monomer containing continuous phase induces meso porosity via either early or late phase separation within the gelation process during the polymerisation [39]. Surfactant concentration and structure also affect the surface area of styrene based polyHIPEs [40]. However, both methods, namely adding porogenic solvent and surfactant to the monomer containing continuous phase increase the nominal porosity which results in sacrificing the material mechanical properties in terms of elastic modulus and brittleness. The morphology of polymers prepared by the addition of porogenic solvents include a fused-bead, cauliflower-like features which is not optimal for mechanical properties [39]. Our study comparing materials with fused-bead and polyHIPE morphology showed that polyHIPE structure is superior to fused-bead morphology allowing for the preparation of materials with overall porosities higher than 75% [32]. Combining high porosity with sufficient mechanical stability is an important materials feature with applications in mind. For example, applying permeable open cellular polyHIPEs for chromatography stationary phases and membranes, significantly higher porosity compared to commercially available monolithic columns facilitated lower back pressures and thus the efficiency of separation [41–50].

## 4. Post polymerisation crosslinking

In order to avoid the formation of fused bead type morphology within the formulating polymer film of the continuous phase of a high internal phase emulsion, a post polymerisation crosslinking of already formed polyHIPE material can be attempted.

Post polymerisation crosslinking, in this description referred to as hypercrosslinking, is a method of polymer chain crosslinking and the result is the creation of numerous new pores at meso and micro size scale thus the creation of meso and/or microporous polymer material [51,52]. The porous profile of hypercrosslinked polymers differs from the porous profile of polymers prepared by free radical polymerisation of monomers and crosslinkers. The porosity of polymers prepared by conventional copolymerisation is the result of phase separation during polymerisation in the presence of an inert diluent, which may be either a non-solvent or a thermodynamically good solvent. The non-solvent does not dissolve the growing crosslinked chains, so the network shrinks and precipitates into micro spheres. These non-porous nodules aggregate and agglomerate in a cauliflower-like structure, and the prepared material is macroporous [53–55]. When a good solvent is used, the polymer network swells, but at high crosslinking degrees it can no longer adsorb the diluent. This results in phase separation in the form of micro and macrosyneresis [56]. In the case of macrosyneresis, a macro porous network is formed as the resulting gel decomposes and thus a microgel is formed, which behaves as a continuous phase in the reaction mixture. These particles then agglomerate during the polymerisation to form a macroporous network. While in microsyneresis the diluent is distributed over the gel. The result of the whole texture is a macroporous network with cauliflower-like structure, but having micro pores due to the primary polymer nodules [53–55]. By using a diluent during radical crosslinking even in the continuous phase of high internal phase emulsions, macroporous materials are obtained. Microsyneresis also introduces micro pores, thus influencing the increase of specific surface area. However, frequently, due to strong capillary forces, the micro pores in polyHIPE collapse during solvent removal.

Unlike traditional crosslinking polymerisation, hypercrosslinked polymers are prepared by post polymerisation crosslinking of long polymer chains in a semi-solution state creating many new bridges. This does not result in phase separation because the polymer chains are distributed throughout the solution and are strongly solvated throughout the hypercrosslinking. A typical example of such process is heating of solvated chloromethylated polystyrene in the presence of a Friedel-Crafts catalyst. This creates new connections by converting chloromethyl groups into methylene bridges that interconnect polymer chains. When the swelling solvent is removed by drying, the additional crosslinking prevents complete collapse of the polymer network and the resulting polymers exhibit extensive microporosity even in the dry state. Initially, the formation of methylene bridges is fast because the mobility of the polymer chains in the swollen polymer is higher than later in the reaction, when the polymer chains are already connected to the newly formed methylene bridges. By introducing new methylene bridges into the network, pores are formed as spaces between highly cross-linked nodules. In further stages of hypercrosslinking, the rigidity of the nodules increases and therefore, after solvent removal, the morphology results in a stable microporous network [52,57]. Hypercrosslinked polymers prepared from gel-type precursors contain only the micro pores. If, on the other hand macroporous polymer is used as the precursor, the product then contains beside the macro pores also micro pores, and a polymer with a bimodal pore distribution is formed. Hypercrosslinked polymers contain a very high density of crosslinks creating micro pores and exhibit high surface areas up to 2000 $m^2/g$ [58,59].

After the removal of the solvent, micro pores remain, which increases compatibility with both polar and non-polar solvents [60,61], what is extremely important for applications. The chemical nature of the conventionally prepared STY / DVB polymer is very similar to the hypercrosslinked polymers that have many methylene bridges between polymer chains. However, these materials differ crucially in terms of topology and mechanical properties. STY / DVB copolymers are prepared without the addition of solvent, which means that their polymer chains are very densely packed in dry state, due to the strong attraction between them. Under these conditions, the polymers swell in thermodynamically good solvents, since the polymer-polymer interactions are replaced by stronger polymer-solvent interactions. Hypercrosslinked polymers, however, are prepared in the presence of an excess of good solvent, and if the crosslinking rate is high and conformational rigid connections are established, then the polymer chains are not densely packed after removal of the solvent. The final material in the dry state has high free volume and significantly reduced polymer-polymer interactions. It is essential that due to the affinity between the polymer fragments, the rigid structure of the hypercrosslinked polymer causes high inner stresses in the polymer chains of the network. Because of this, the hypercrosslinked materials tend to release inner stresses, which happens when the network is expanded, that is, when it swells. Swelling is possible on contacting any liquid, regardless of thermodynamic affinity with the polymer which means that the hypercrosslinked polymers are compatible with both thermodynamically good and bad solvents [60,62].

Hypercrosslinking can be achieved by different chemical methods and can be divided into: post polymerisation crosslinking (hypercrosslinking using polystyrene precursors, hypercrosslinking using VBC / DVB precursors), direct one-step polycondensation of functional monomers and hypercrosslinking by the so called *knitting* method.

### 4.1. Hypercrosslinking of polystyrene precursurs (*Davankov* resins)

Introduction of hypercrosslinking of polymer chains dates into 70’s when hypercrosslinked polystyrene (PS) was demonstrated, using linear PS or gel-type swollen polystyrene-co-divinylbenzene and external crosslinkers in the presence of Lewis acid catalyst and solvents [63]. External crosslinkers create new covalent bonds between polystyrene chains applying the Friedel-Crafts reaction [61,64,65] (Scheme 1). This reaction achieves short and rigid connections and forms a rigid three-dimensional polymer network. Almost all aromatic rings can be consumed in this reaction, which results in a high degree of hypercrosslinking, and consequently in a large number of newly formed links and a high specific surface area of the materials [51]. Typical protocol for hypercrosslinking of linear polystyrene or the STY / DVB copolymer contains introducing a sufficient amount of external crosslinker into the dissolved linear polystyrene or swollen polystyrene network and adding the Lewis acid while cooling the reaction medium to achieve homogeneous distribution of the catalyst before gelation of the mixture. The mixture is then heated, allowing high conversion of the reactive linker groups [66]. As external linkers, chloroalkanes are most commonly used; usually dichloroethane, as it plays two roles - as an external linker and a good solvent for PS.

Chloromethyl ether was used predominantly for the hypercrosslinking of polystyrene, but was replaced by monochlorodimethyl ether [60,67–69], carbon tetrachloride [70,71], dichloroxylene [64,72], 4,4'-bis (chloromethyl)-biphenyl [64,72], trifunctional tris-(chloromethyl)-mesitylene [51], 4,4'-bis-chloromethyl-1,4-diphenylbutane [51], formaldehyde dimethyl acetal [71–74] or dichloroethane [51,75,76] and other dichloroalkanes [76], due to its adverse health effects. It should be noted that the length of the external crosslinker affects the rigidity of the hypercrosslinked material, which also affects the morphology of the material. All the compounds form bridges of a limited conformational mobility in the final network except for diphenylbutane. In this case, the diphenylmethane crosslinker type are most influenced by the rigidity of the structure. Another limitation in mobility is tris- (chloromethyl) -mesitylene because it links three polystyrene chains at one point.

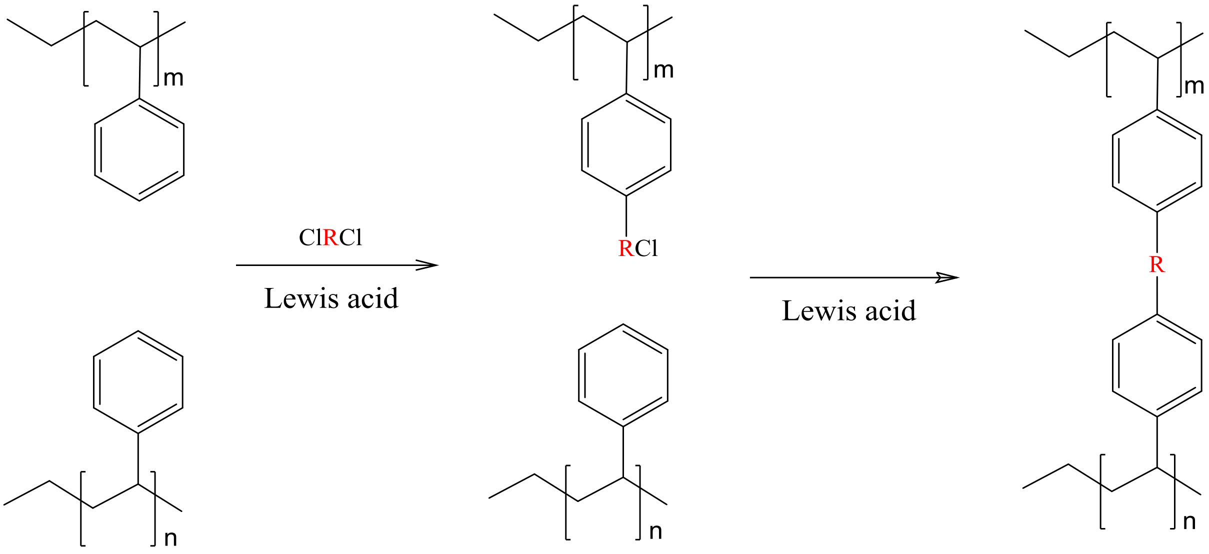

**Scheme 1:** Post polymerisation hypercrosslinking : Hypercrosslinking using polystyrene precursurs (*Davankov* resins)

When PS with a low degree of initial crosslinking (0.3-2%) is used for hypercrosslinking, intrinsic microporosity is formed. However, if the initial degree of crosslinking is increased, the macroporous network is formed prior to hypercrosslinking, so the final pore distribution is bimodal [61,77].

Due to their high surface area, good solvent compatibility and good mechanical properties, bimodal porosity and interpenetrating network, hypercrosslinked polystyrenes are often used as adsorbents for gases [78,79] and various organic molecules [57,80,81], for chromatographic separation [82–84], or for adsorbents for blood purification [85].

## 4.2. Hypercrosslinking using chloromethylated groups of vinylbenzyl chloride

Hypercrosslinking can be performed on polyvinylbenzyl chloride or its copolymers utilizing vinylbenzyl chloride moieties in the polymer chains as internal electrophiles in the Friedel-Crafts reaction, without the addition of external linkers (**Scheme 2**) [58,61]. In this reaction, the chloromethyl groups are converted to methylene bridges and thus new links are created. The aromatic ring which is to be substituted is electron-rich, resulting in a formation of six-membered ring following the cyclization reaction. As with Davankov's type of hypercrosslinking, $FeCl_3$ is most commonly used as a Friedel-Crafts catalyst because it is has good solubility in the usual solvents used and does not cause steric hindrance [58]. Due to the similarity of the polystyrene network to VBC / DVB network, the same solvents are used, most commonly DCE. The morphology of polymers hypercrosslinked by this post-polymerisation approach is similar to *Davankov* type resins meaning that hypercrosslinking induces micro pores and results in a significant increase of specific surface area. This was demonstrated by hypercrosslinking several poly (VBC-DVB) copolymers with DVB content between  2% and 20% [58]. The specific surface area of hypercrossliked products depended on the initial crosslinking and reaction time, being highest with lowest initial crosslinking and increasing with reaction time up to 2 hours while further elongation of reaction time had no effect. Decrease in the chloride content of the polymer coincides with the drastic increase in the specific surface area.

The importance of initial crosslinking for efficiency of hypercrosslinking and final porous structure was confirmed in another report. [86] The maximum specific surface area was achieved after hypercrosslinking of polymer containing 2% of DVB (2060 $m^2/g$). By increasing the DVB amount, a bimodal structure was formed, with well-defined macro and micro pores, while at 7% of DVB the structure was completely micro porous. Increasing the surface area after hypercrosslinking of VBC/DVB polymers at a lower DVB content occurs because the macromolecular chains of the polymer are still very loose and can orient more favorably in the presence of solvent in the hypercrosslinking process, thus forming more methylene bridges than in the case of higher crosslinked poly (VBC / DVB).

One of the most advantageous consequences of hypercrosslinking VBC / DVB polymers is their improved sorption properties. Unlike non-functionalized hypercrosslinked polystyrene, which is a good sorbent due to hydrophobic π-π interactions [82], functional groups can undoubtedly improve the adsorption properties, which in turn can affect the development of many applications [87–91].

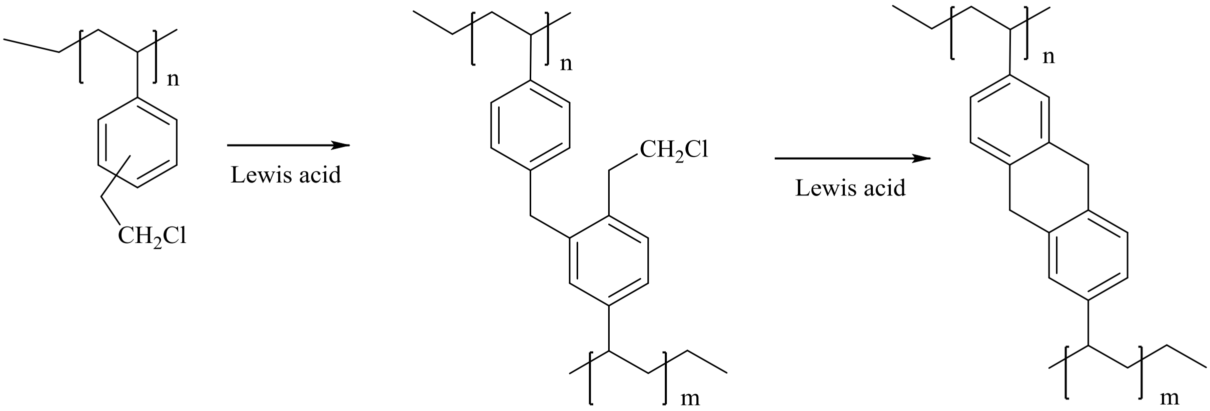

**Scheme 2:** Post polymerisation hypercrosslinking : Hypercrosslinking using chloromethylated groups of vinylbenzyl chloride

### 4.3. Direct hypercrosslinking arising from polycondensation

Hypercrosslinked polymers can also be produced by the direct polycondensation of small molecule monomers without the need to make the precursor crosslinked polymer. However, the synthesis of polymer precursors is time-consuming and limited functional monomers can be selected to satisfy the combined conditions from reactions of radical polymerisation and Friedel–Crafts alkylation. Similarly to the other hypercrosslinking approaches these use DCE as a solvent and $FeCl_3$ as a Friedel-Crafts catalysts. The resulting networks can be considered the analogues of the Friedel-Crafts linked PS materials. This direct approach creates microporous organic networks and uses bis(chloromethyl) aromatic monomers such as dichloroxylene [92], bis(chloromethyl)biphenyl [75,93], and bis(chloromethyl) anthracene [75,93]. By using Lewis acid as a catalyst, the chloromethylene groups react with adjacent phenyl rings. This results in the formation of rigid methylene bonds between the rings, which in turn produces micro pores and high specific surface areas up to 2000 $m^2/g$ [93]. Due to high specific surface areas hypercrosslinked polymers using polycondensation have good gas adsorption capacity [75,93–95]. The use of *o*-DCX isomers for condensation with *m*-DCX or *p*-DCX has been found to have an adverse effect on the growth of specific surface areas, while *m*-DCX and *p*-DCX provide materials with comparable specific surface areas [75]. For well-defined micro porous polymers, DCX and BCMBP were used as crosslinkers in order to connect heterocyclic (carbazole), metal-doped (ferrocene) and highly rigid (triptycene) building blocks. It was also found that the length of crosslinkers can affect the porosity of the resulting polymer. For example, longer crosslinker molecules affect larger pores, while shorter molecules create micro pores, thereby contributing to an increase in the specific surface area of the polymer [96]. Fluorene derivatives (fluorene, 9,90-spirobi(fluorene), dibenzofuran and dibenzothiophene) were also used as non-functional aromatic precursors, which showed good microstructure in condensation with BCMBP under Friedel-Crafts catalytic conditions. The highest surface area of up to 1800 $m^2/g$ was obtained from dibenzofurane monomers with 10% molar fraction [95].

Aromatic precursors used in addition to benzene [97,98] were polyaniline [95], polypyrrole [94], polythiophene, polyfurane, aniline, carbazole [99,100], aminobenzene [101], bishydroxymethyl monomers [102], and were found to form hypercrosslinked polymers.

### 4.4. Knitting aromatic compound polymers using an external crosslinker

A special type of one-step polycondensation, however, is the “knitting” method for hypercrosslinking with an external crosslinker-formaldehyde dimethyl acetal FDA, which is more environmentally friendly as it has no dangerous by-products during the Friedel-Crafts reaction. The mechanism of the reaction is proposed as: Lewis acid first complexes with the crosslinking molecule, which reduces the interaction between the methoxyl group and the central carbon atom, and then produces a large number of intermediate carbocations in the DCE (Scheme 3) [98]. The carbocations then react with the phenyl ring and the addition of the multi - methoxymethyl groups to the aromatic ring proceeds, releasing methanol. The methoxymethyl groups are then converted to methylene links and reacted with other phenyl rings to form a rigid crosslinked structure.

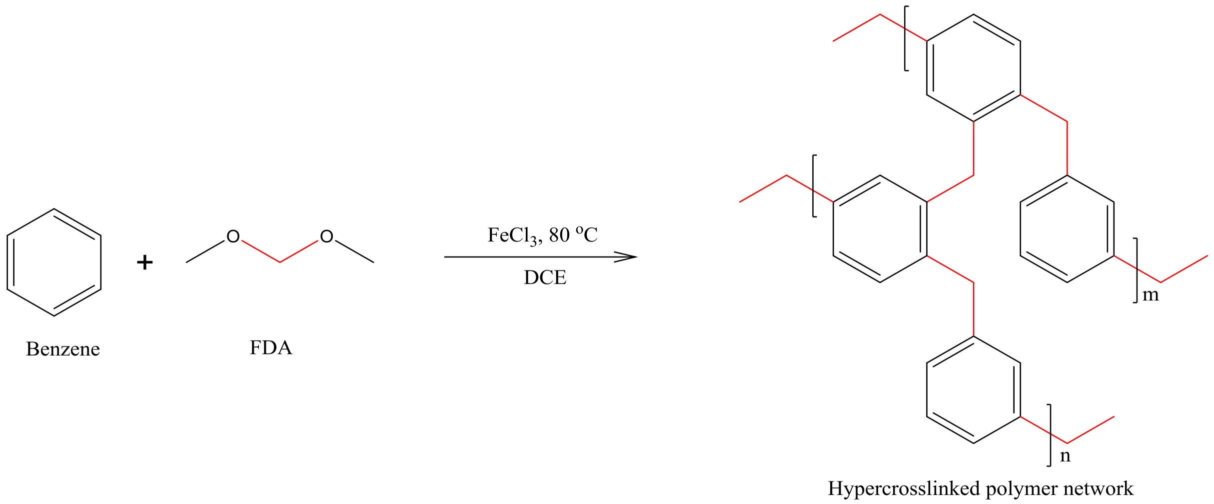

**Scheme 3:** Typical hypercrosslinking by the knitting method from benzene monomers [98]

Typically, in this one-step approach, the aromatic monomer (including benzene, phenol or chlorobenzene), the crosslinker (FDA) and the catalyst ($FeCl_3$) are dissolved in DCE to complete the condensation [98]. Increasing the FDA crosslinker content of hypercrosslinked materials obtained using tetraphenylmethane blocks also increases the specific surface area up to 1314 $m^2/g$ [103]. Similar approaches using FDA as external crosslinker were shown with different monomers such as aromatic heterocycles [104,105], hydroxymethylated aromatic molecules [102], aniline and benzene [72,97], styrene [105] and tetrahedral monomers [106,107], among others. The "knitting" method is used for the design and synthesis of microporous polymers based on various rigid aromatic building blocks, including nonhalogenated monomers. 1,4-dimethoxybenzene was also used as an external crosslinker [108].

## 5. Hypercrosslinking of polyHIPEs

Hypercrosslinking of polyHIPE polymers results in rigid polymers with induced meso and microporosity (tertiary pores) in macroporous material which leads to very high specific surface areas due to induction of micro and meso pores. Research so far shows that the morphology of polyHIPEs does not change significantly after hypercrosslinking and the typical open cellular macroporous structure is retained [59]. Rigid connections created during hypercrosslinking make better compatibility with both thermodynamically good and bad solvents and thus better accesibility of reactive sites. As a result, hierarchically porous material is obtained which has macro pores that allow convective transfer of the substance and reduce back pressure in flow systems, and at the same time has a very high specific surface area due to the presence of micro and meso pores and also has good accessibility to reactive sites in the material. PolyHIPEs with hierarchical or bimodal porosity are very useful in many applications as demonstrated by various research groups.

Schwab et al. [77] synthesized VBC / DVB polyHIPE monoliths, and the DVB molar fraction varied between 2.5 and 40%. Materials were hypercrosslinked by Friedel-Crafts alkylation reaction in the presence of a Lewis base to give monoliths with specific surface areas up to 1200 $m^2/g$, while maintaining the morphology of precursor polyHIPE. Due to hypercrosslinking, the non-porous walls of polyHIPEs have become highly microporous. Such monolithic VBC based polyHIPE polymers with bimodal structure were proven to be very promising for n-butane storage and the results were comparable to the commercially available Sorbonorit powder. In another report, VBC based polyHIPEs with 2 mol% DVB content were used for controlled hypercrosslinking to leave some unreacted benzyl chloride groups for further binding of methyl amino pyridine. Functionalized hypercrosslinked polyHIPE was used as a very effective nucleophilic catalyst for the alkylation of methylcyclohexanol with acetic anhydride due to its hierarchical porosity and high specific surface area. It was found that after 3 hours, 100% alkylation conversion was achieved using hypercrosslinked polyHIPE-MAP while non hypercrosslinked materials performed significantly worse demonstrating the advantage of the bimodal pore structure with facilitated mass transfer [59].

In addition to hypercrosslinking styrene type polyHIPEs with an internal crosslinker, Friedel-Crafts reaction with an external crosslinker was used. Crosslinked STY / DVB polyHIPEs were used for hypercrosslinking using formaldehyde dimethyl acetal as the external crosslinker applying the knitting approach. This hypercrosslinking method resulted in polyHIPE monoliths with specific surface areas between up to 595 $m^2/g$. Due to their extremely hydrophobic surface, the hypercrosslinked STY / DVB polyHIPE materials have shown good absorption capacity for oils, and could be used for oil-spill cleaning [109].

Knitting type hypercrosslinking was also used to synthesize porous carbon foams, which were produced by carbonizing the STY / DVB hypercrosslinked polyHIPEs. Dimethoxymethane was used as an external crosslinker for hypercrosslinking. It was found that the STY / DVB ratio of polyHIPE precursors is strongly influenced by char yield, micro pore volume and BET surface area of carbonized polyHIPEs [110].

Silverstein et al. synthesized porous carbons with high specific surface areas and hierarchical porous structure by pyrolysis of hypercrosslinked VBC / DVB polyHIPEs. [111] Hypercrosslinking generated new links which limited the degradation of polyHIPE morphology after pyrolysis. Surface areas of pyrolyzed hypercrosslinked polyHIPEs were as high as 553 $m^2/g$, which meant less than 40% reduction compared to precursor polymers. Hypercrosslinking via $FeCl_3$ catalysis was further used to synthesize acrylonitrile-DVB polyHIPEs, which were used for pyrolysis to produce nitrogen- and oxygen-codoped carbo-polyHIPEs with interconnected macro pores and micro / mesoporous carbon skeleton [112]. Such carbo-polyHIPE was applied as a solid state support for Pt and Ru bimetal nanoparticles, which, in turn, demonstrated a remarkable electrocatalytic ability to methanol electrooxidation. The specific surface area of carbo-HIPE was increased to 417 $m^2/g$ after hypercrosslinking, which proved to be important for improving electrocatalytic performance. Silica particle stabilized polyDVB polyHIPE was used as a porous solid acid catalyst for the production of hydroxymethyl furfural from cellulose in the presence of 1-ethyl-3-methyl-imidazolium chloride. For comparison, basic polyDVB was prepared, grafted with a $-SO_3H$ sulfonation process, and PDVB-co-SS polyHIPE, which was also sulfonated. This polymer was then hypercrosslinked and used as a solid state catalyst which, in addition to the macro pores in its skeleton, also had micro pores and, consequently, high specific surface area. Large specific surface area of polyHIPE and super-strong acid sites have been found to be crucial for cellulose conversion [113]. Sevšek et al. [114] synthesized STY / DVB polyHIPE monoliths with high DVB content. The remaining vinyl groups of DVB in STY / DVB monoliths were used for post-polymerisation crosslinking using the radical initiator di-tert-butyl peroxide in toluene and acetonitrile. The surface area in both solvents was found to be much larger after hypercrosslinking (up to 355 $m^2/g$), and the nitrogen adsorption / desorption method showed an increase in the number of micro pores after hypercrosslinking, which coincides with an increase in specific surface area. Pyridine containing polyHIPE could be hypercrosslinked by the second stage radical crosslinking of remaining vinyl groups [115]. For the purposes of solid state support for catalysts, vinyl pyridine-DVB polyHIPE was prepared. Pyridine ring nitrogen was used for further functionalization — for the Cu (II) coordinate linker. This functionalized polyHIPE has been used as a solid state support for catalysts for a cycloaddition click reaction. Post polymerisation radical treatment (using di-tert-butyl peroxide) increased the specific surface area and created a multi modal porous profile, which was crucial for the success of the cycloaddition reaction.

Hypercrosslinking was demonstrated also on non styrene-type polyHIPEs. Mezhoud et al. [116] synthesized poly (2-hydroxyethyl methacrylate-co-N,N'-methylenebisacrylamide) polyHIPE and functionalized it with allylamine and propagylamine to create free double bonds that were used for hypercrosslinking with di- or tetra-thiols via thiol-ene click reactions. After the treatment surface areas of up to 1500 $m^2/g$ ware measured. The monoliths were then used for Au-nanoparticle decorated catalytic support to reduce nitrophenol and Eosin Y.

Another similar method is described as *in situ* hypercrosslinking of GMA-based polyHIPEs with multifunctional amines, where the amino-epoxy reaction is running parallel to the polymerisation. The result is a highly porous material with surface areas up to 63 $m^2/g$ and with good accessibility of reactive sites, but this system has disadvantages in terms of HIPE stability [117].

## 6. Conclusion and outlook

Porous polymers in different formats e.g. particles, monoliths, membranes, have a wide range of application fields, in separation, catalysis, synthesis, purification, in biomedical fields as supports for cell and tissue cultivation etc. Control of pore geometry, interconnectivity and size is of utmost importance for the desired performance. While there are many methods for creating macroporosity in polymers, either during the polymerisation or after, high internal phase emulsion templating offers easily scalable straightforward technique for the synthesis of polymers with spherical interconnected pores with micrometer dimensions and high pore volume. Polymerisation parameters, droplet phase volume share and surfactants are key factors deciding the final structure. While good control of macroporosity in polyHIPEs is possible, the introduction of meso and microporosity is less trivial. Addition of porogenic solvents into the continuous phase can induce meso and micro porosity however the prevalence of cauliflower-like morphology and increase of pore volume significantly decreases the mechanical properties and is therefore in many cases unpractical. On the other hand, the post polymerisation hypercrosslinking enables the creation of meso and microporosity in already formed macroporous polyHIPEs without sacrificing the mechanical properties or even improving them in many aspects. Improved accessibility of reactive sites in the interior of the bulk of the material, increased surface area and wide solvent compatibility are further advantages of hypercrosslinked polyHIPEs. It is therefore expected that such materials with bimodal and hierarchical pore distribution will play an increasingly important role in various application fields in the future.

[1] A. Wilkinson, A. McNaught, *Compendium Of Chemical Terminology (″Gold Book″)*, Blackwell Scientific Publications, Oxford, UK, **1997**.

[2] M. S. Silverstein, Polymer **2014**, *55*, 304–320.

[3] M. S. Silverstein, Polymer **2017**, *126*, 261–282.

[4] Y. Huang, S. H. Kim, L. R. Arriaga, *Adv. Colloid Interface Sci.* **2017**, *247*, 413–425.

[5] B. F. B. Silva, C. Rodríguez-Abreu, N. Vilanova, *Curr. Opin. Colloid Interface Sci.* **2016**, *25*, 98–108.

[6] N. R. Cameron, Polymer **2005**, *46*, 1439–1449.

[7] I. Pulko, P. Krajnc, *Encycl. Polym. Sci. Technol.* **2017**, 1–28, DOI: 10.1002/0471440264.pst653.

[8] R. Foudazi, S. Qavi, I. Masalova, A. Y. Malkin, *Adv. Colloid Interface Sci.* **2015**, *220*, 78–91.

[9] D. Barby and Z. Haq, *Low Density Porous Cross-Linked Polymeric Material Sand Their Preparation*, **1986,** EP Pat 60138.

[10] S. Kovačič, D. Štefanec, P. Krajnc, *Macromolecules* **2007**, *40*, 8056–8060.

[11] I. Pulko, P. Krajnc, *Macromol. Rapid Commun.* **2012**, *33*, 1731–46.

[12] E. Kot, N. Shirshova, A. Bismarck, J. H. G. Steinke, *RSC Adv.* **2014**, *4*, 11512.

[13] P. Krajnc, D. Štefanec, I. Pulko, *Macromol. Rapid Commun.* **2005**, *26*, 1289–1293.

[14] S. Kovačič, D. Štefanec, P. Krajnc, *Macromolecules* **2007**, *40*, 8056–8060.

[15] J. Majer, M. Paljevac, E. Žagar, S. Kovačič, P. Krajnc, *React. Funct. Polym.* **2016**, *109*, 99–103.

[16] M. Paljevac, K. Jeřabek, P. Krajnc, *J. Polym. Environ.* **2012**, *20*, 1095–1102.

[17] O. Kulygin, M. S. Silverstein, *Soft Matter* **2007**, *3*, 1525–1529.

[18] M. Ovadia, M. S. Silverstein, *Polym. Int.* **2016**, *65*, 280–289.

[19] B. H. L. Oh, A. Bismarck, M. B. Chan-Park, *J. Mater. Chem. B* **2015**, *3*, 4118.

[20] N. C. Grant, A. I. Cooper, H. Zhang, *ASC Appl. Mater. Interface* **2010**, *2*, 1400–1406.

[21] R. Butler, I. Hopkinson, A. I. Cooper, *J. Am. Chem. Soc.* **2003**, *125*, 14473–14481.

[22] F. Audouin, M. Birot, E. Pasquinet, O. Besnard, P. Palmas, D. Poullain, H. Deleuze, *Macromolecules* **2011**, *44*, 4879–4886.

[23] C. Youssef, R. Backov, M. Treguer, M. Birot, H. Deleuze, *J. Polym. Sci. Pt A Polym. Chem.* **2010**, *48*, 2942–2947.

[24] D. Golub, P. Krajnc, *React. Funct. Polym.* **2020**, *149*, 104515.

[25] M. Sušec, S. C. Ligon, J. Stampfl, R. Liska, P. Krajnc, *Macromol. Rapid Commun.* **2013**, *34*, 938–943.

[26] D. W. Johnson, C. Sherborne, M. P. Didsbury, C. Pateman, N. R. Cameron, F. Claeyssens, *Adv. Mater.* **2013**, *25*, 3177–3177.

[27] C. E. Hoyle, C. N. Bowman, *Polym. Chem.* **2010**, *49*, 1540–1573.

[28] A. Galperin, K. Smith, N. S. Geisler, J. D. Bryers, B. D. Ratner, *ACS Biomater. Sci.* **2015**, *1*, 593–600.

[29] H. B. Ly, L. Halbardier, D. Grande, *Macromol. Symp.* **2016**, *365*, 49–58.

[30] R. B. Diego, M. P. Olmedilla, A. S. Aroca, J. L. G. Ribelles, M. M. Pradas, G. G. Ferrer, M. S. Sanchez, *J. Mater. Sci.* **2005**, *40*, 4881–4887.

[31] T. J. Long, C. C. Sprenger, S. R. Plymate, B. D. Ratner, *Biomaterials* **2014**, *35*, 8164–8174.

[32] M. Paljevac, L. Gradišnik, S. Lipovšek, U. Maver, J. Kotek, P. Krajnc, *Macromol. Biosci.* **2018**, *18*, 1–8.

[33] N. Bhardwaj, S. C. Kundu, *Biotechnol. Adv.* **2010**, *28*, 325–347.

[34] L. Wang, A. J. Ryan, *Electrospinning Tissue Regen.* **2011**, 3–33.

[35] A. Samanta, B. Nandan, R. K. Srivastava, *J. Colloid Interface Sci.* **2016**, DOI 10.1016/j.jcis.2016.03.012.

[36] B. A. Dikici, S. Dikici, G. C. Reilly, S. MacNeil, F. Claeyssens, *Materials (Basel).* **2019**, *12*, DOI 10.3390/ma12162643.

[37] N. R. Cameron, A. Barbetta, *J. Mater. Chem.* **2000**, *10*, 2466–2471.

[38] J. M. Williams, A. J. Gray, M. H. Wilkerson, *Langmuir* **1990**, *6*, 437–444.

[39] D. C. Sherrington, P. Hodge, *Synthesis Separations Using Functional Polymers*, Wiley-VCH Verlag GmbH&Co. KGaA, **1988**.

[40] A. Barbetta, N. R. Cameron, *Macromolecules* **2004**, *37*, 3202–3213.

[41] S. Huš, M. Kolar, P. Krajnc, *J. Chromatogr. A* **2016**, *1437*, 168–175.

[42] P. Krajnc, N. Leber, D. Štefanec, S. Kontrec, A. Podgornik, *J. Chromatogr. A* **2005**, *1065*, 69–73.

[43] S. Jerenec, M. Šimić, A. Savnik, A. Podgornik, M. Kolar, M. Turnšek, P. Krajnc, *React. Funct. Polym.* **2014**, *78*, 32–37.

[44] M. Tebboth, A. Menner, A. Kogelbauer, A. Bismarck, *Curr. Opin. Chem. Eng.* **2014**, *4*, 114–120.

[45] J. Pribyl, B. Fletcher, W. Steckle, K. Taylor-Pashow, T. Shehee, B. Benicewicz, *Anal. Chem.* **2017**, *89*, 5174–5178.

[46] K. M. L. Taylor-Pashow, J. G. Pribyl, *Solvent Extr. Ion Exch.* **2019**, *37*, 1–26.

[47] D. Yin, Y. Guan, H. Gu, Y. Jia, Q. Zhang, *RSC Adv.* **2017**, *7*, 7303.

[48] J. Majer, P. Kranjc, *Macromol. Symp.* **2010**, *296*, 5–10.

[49] J. M. Hughes, P. M. Budd, K. Tiede, J. Lewis, *J. Apply. Polym. Sci.* **2014**, *132*, 41229.

[50] S. Choudhury, L. Fitzhenry, B. White, D. Connolly, *Materials (Basel).* **2016**, *9*, 1–14.

[51] V. A. Davankov, M. P. Tsyurupa, *React. Polym.* **1990**, *13*, 27–42.

[52] M. P. Tsyurupa, V. A. Davankov, *React. Funct. Polym.* **2002**, *53*, 193–203.

[53] O. Okay, *Prog. Polym. Sci.* **2000**, *25*, 711–779.

[54] M. P. Tsyurupa, V. A. Davankov, *React. Funct. Polym.* **2006**, *66*, 768–779.

[55] D. C. Sherrington, *Chem. Commun.* **1998**, 2275–2286.

[56] K. Dušek, *J. Polym. Sci. Part C Polym. Symp.* **2010**, *16*, 1289–1299.

[57] P. Veverka, K. Jeřábek, *React. Funct. Polym.* **2004**, *59*, 71–79.

[58] J. H. Ahn, J. E. Jang, C. G. Oh, S. K. Ihm, J. Cortez, D. C. Sherrington, *Macromolecules* **2006**, *39*, 627–632.

[59] I. Pulko, J. Wall, P. Krajnc, N. R. Cameron, *Chem. Eur. J.* **2010**, *16*, 2350–2354.

[60] A. V. Pastukhov, M. P. Tsyurupa, V. A. Davankov, *J. Polym. Sci. Pt B Polym. Phys.* **1999**, *37*, 2324–2333.

[61] P. Veverka, K. Jeřábek, *React. Funct. Polym.* **1999**, *41*, 21–25.

[62] V. A. Davankov, M. P. Tsyurupa, *React. Polym.* **1990**, *13*, 27–42.

[63] V. Davankov, V. Rogozhin, M. Tsyurupa, *Macronet Polystyrene Structures for Ionites and Method of Producing Same*, **1969,** US Pat 3729457.

[64] V. A. Davankov, S. V. Rogoshin, M. P. Tsyurupa, *J Polym Sci Part C, Polym Symp* **1974**, *101*, 95–101.

[65] V. A. Davankov, G. I. Timofeeva, M. M. Ilyin, M. P. Tsyurupa, *J. Polym. Sci. Part A Polym. Chem.* **1997**, *35*, 3847–3852.

[66] V. Davankov, M. Tsyurupa, *Compr. Anal. Chem.* **2011**, *56*, 166–193.

[67] M. P. Tsyurupa, Z. K. Blinnikova, Y. A. Davidovich, S. E. Lyubimov, A. V. Naumkin, V. A. Davankov, *React. Funct. Polym.* **2012**, *72*, 973–982.

[68] M. P. Tsyurupa, A. V. Pastukhov, V. A. Davankov, *Dokl. Akad. Nauk* **1997**, *352*, 2324–2333.

[69] V. A. Davankov, M. M. Ilyin, M. P. Tsyurupa, G. I. Timofeeva, L. V. Dubrovina, *Macromolecules* **1996**, *29*, 8398–8403.

[70] J. Hradil, E. Králová, Polymer **1998**, *39*, 6041–6048.

[71] D. Zhang, L. Tao, J. Ju, Y. Wang, Q. Wang, T. Wang, Polymer **2015**, *60*, 234–240.

[72] F. Maya, F. Svec, Polymer **2014**, *55*, 340–346.

[73] T. Ratvijitvech, M. Barrow, A. I. Cooper, D. J. Adams, *Polym. Chem.* **2015**, *6*, 7280–7285.

[74] L. Tan, B. Li, X. Yang, W. Wang, B. Tan, Polymer **2015**, *70*, 336–342.

[75] C. D. Wood, T. Bien, A. Trewin, N. Hongjun, D. Bradshaw, M. J. Rosseinsky, Y. Z. Khimyak, N. L. Campbell, R. Kirk, E. Stöckel, A. I. Cooper, *Chem. Mater.* **2007**, *19*, 2034–2048.

[76] M. Ghafari, J. D. Atkinson, Polymer **2017**, *116*, 278–286.

[77] M. G. Schwab, I. Senkovska, M. Rose, N. Klein, M. Koch, J. Pahnke, G. Jonschker, B. Schmitz, M. Hirscher, S. Kaskel, *Soft Matter* **2009**, *5*, 1055–1059.

[78] Y. Yang, B. Tan, C. D. Wood, *J. Mater. Chem. A* **2016**, *4*, 15072–15080.

[79] Q. Liu, B. Xia, J. Huang, B. Liao, H. Liu, B. Ou, L. Chen, Z. Zhou, *Mater. Chem. Phys.* **2017**, *199*, 616–622.

[80] L. D. Belyakova, T. I. Schevchenko, V. A. Davankov, M. P. Tsyurupa, *Adv. Colloid Interface Sci.* **1986**, *25*, 249–266.

[81] M. P. Tsyurupa, L. A. Maslova, A. I. Andreeva, T. A. Mrachkovskaya, V. A. Davankov, *React. Polym.* **1995**, *25*, 69–78.

[82] N. A. Penner, P. N. Nesterenko, M. M. Hyin, M. P. Tsyurupa, V. A. Davankov, *Chromatographia* **1999**, *50*, 611–620.

[83] V. Davankov, M. Tsyurupa, M. Ilyin, L. Pavlova, *J. Chromatogr. A* **2002**, *965*, 65–73.

[84] V. A. Davankov, C. S. Sychov, M. M. Ilyin, K. O. Sochilina, *J. Chromatogr. A* **2003**, *987*, 67–75.

[85] V. Davankov, L. Pavlova, M. Tsyurupa, J. Brady, M. Balsamo, E. Yousha, *J. Chromatogr. B Biomed. Sci. Appl.* **2000**, *739*, 73–80.

[86] B. Li, R. Gong, Y. Luo, B. Tan, *Soft Matter* **2011**, *7*, 10910.

[87] J. Urban, F. Svec, J. M. J. Fréchet, *J. Chromatogr. A* **2010**, *1217*, 8212–8221.

[88] J. Urban, F. Svec, J. M. J. Fréchet, *Anal. Chem.* **2010**, *82*, 1621–1623.

[89] Y. Lv, Z. Lin, F. Svec, *Anal. Chem.* **2012**, *84*, 8457–8460.

[90] X. J. Chen, N. P. Dinh, J. Zhao, Y. T. Wang, S. P. Li, F. Svec, *J. Sep. Sci.* **2012**, *35*, 1502–1505.

[91] F. Maya, F. Svec, *J. Chromatogr. A* **2013**, *1317*, 32–38.

[92] Z. K. Blinnikova, I. R. Golding, M. P. Tsyurupa, A. A. Fomkin, A. L. Pulin, V. A. Davankov, *Polym. Sci. - Ser. B* **2018**, *60*, 91–98.

[93] C. D. Wood, B. Tan, A. Trewin, F. Su, M. J. Rosseinsky, D. Bradshaw, Y. Sun, L. Zhou, A. I. Cooper, *Adv. Mater.* **2008**, *20*, 1916–1921.

[94] J. Germain, J. M. J. Fréchet, F. Svec, *Chem. Commun.* **2009**, 1526–1528.

[95] M. G. Schwab, A. Lennert, J. Pahnke, G. Jonschker, M. Koch, I. Senkovska, M. Rehahn, S. Kaskel, *J. Mater. Chem.* **2011**, *21*, 2131–2135.

[96] D. Chen, S. Gu, Y. Fu, Y. Zhu, C. Liu, G. Li, G. Yu, C. Pan, *Polym. Chem.* **2016**, *7*, 3416–3422.

[97] R. Dawson, T. Ratvijitvech, M. Corker, A. Laybourn, Y. Z. Khimyak, A. I. Cooper, D. J. Adams, *Polym. Chem.* **2012**, *3*, 2034–2038.

[98] B. Li, R. Gong, W. Wang, X. Huang, W. Zhang, H. Li, C. Hu, B. Tan, *Macromolecules* **2011**, *44*, 2410–2414.

[99] L. Pan, Q. Chen, J.-H. Zhu, J.-G. Yu, Y.-J. He, B.-H. Han, *Polym. Chem.* **2015**, *6*, 2478–2487.

[100] X. Yang, M. Yu, Y. Zhao, C. Zhang, X. Wang, J. X. Jiang, *RSC Adv.* **2014**, *4*, 61051–61055.

[101] J. Germain, F. Svec, J. M. J. Fre´chet, *Chem. Mater.* **2008**, *20*, 7069–7076.

[102] Y. Luo, S. Zhang, Y. Ma, W. Wang, B. Tan, *Polym. Chem.* **2013**, *4*, 1126–1131.

[103] M. L. Errahali M., Gatti G., Tei L., Paul G., Rolla G. A., Canti L., Fraccarollo A., Cossi M., Comotti A., Sozzani P., *J. Phys. Chem.* **2014**, *118*, 28699–28710.

[104] Y. Luo, B. Li, W. Wang, K. Wu, B. Tan, *Adv. Mater.* **2012**, *24*, 5703–5707.

[105] T. Ratvijitvech, M. Barrow, A. I. Cooper, D. J. Adams, *Polym. Chem.* **2015**, *6*, 7280–7285.

[106] S. Yao, X. Yang, M. Yu, Y. Zhang, J. X. Jiang, *J. Mater. Chem. A* **2014**, *2*, 8054–8059.

[107] R. Dawson, E. Stöckel, J. R. Holst, D. J. Adams, A. I. Cooper, *Energy Environ. Sci.* **2011**, *4*, 4239–4245.

[108] L. Tan, B. Li, X. Yang, W. Wang, B. Tan, Polymer **2015**, *70*, 336–342.

[109] X. Yang, L. Tan, L. Xia, C. D. Wood, B. Tan, *Macromol. Rapid Commun.* **2005**, *36*, 1553–1558.

[110] R. T. Woodward, A. Jobbe-Duval, S. Marchesini, D. B. Anthony, C. Petit, A. Bismarck, Polymer **2017**, *115*, 146–153.

[111] S. Israel, I. Gurevitch, M. S. Silverstein, Polymer **2015**, *72*, 453–463.

[112] F. Yi, Y. Gao, H. Li, L. Yi, D. Chen, S. Lu, *Electrochim. Acta* **2016**, *211*, 768–776.

[113] J. Pan, H. Gao, Y. Zhang, J. Zeng, W. Shi, C. Song, Y. Yan, L. Yu, D. Chang, *RSC Adv.* **2014**, *4*, 59175–59184.

[114] U. Sevšek, J. Brus, K. Jeřabek, P. Krajnc, Polymer **2014**, *55*, 410–415.

[115] A. Koler, M. Paljevac, N. Cmager, J. Iskra, M. Kolar, P. Krajnc, Polymer **2017**, *126*, 402–407.

[116] S. Mezhoud, M. Paljevac, A. Koler, B. Le Droumaguet, D. Grande, P. Krajnc, *React. Funct. Polym.* **2018**, *132*, 51–59.

[117] J. Majer, E. Žagar, P. Krajnc, S. Kovačič, *Colloid Polym. Sci.* **2019**, *297*, 239–247.